Published in final edited form as:

Schizophr Res. 2019 August ; 210: 107–114. doi:10.1016/j.schres.2019.05.039.

White matter development in infants at risk for schizophrenia

Sung Jun Ahn[1], **Emil Cornea**[2], **Veronica Murphy**[2], **Martin Styner**[2,3], **L. Fredrik Jarskog**[2], **John H. Gilmore**[2]

[1]Department of Radiology, Yonsei University College of Medicine, Seoul 06273, Korea

[2]Department of Psychiatry, University of North Carolina at Chapel Hill, Chapel Hill, 27599-7160, USA

[3]Department of Computer Science, University of North Carolina, Chapel Hill, NC 27599, USA

Abstract

Background: Schizophrenia is considered a neurodevelopmental disorder with a pathophysiology that likely begins long before the onset of clinical symptoms. White matter abnormalities have been observed in schizophrenia and we hypothesized that the first 2 years of life is a period in which white matter abnormalities associated with schizophrenia risk may emerge.

Methods: 38 infants at high risk for schizophrenia and 202 healthy controls underwent diffusion tensor MRIs after birth and at 1 and 2 years of age. Quantitative tractography was used to determine diffusion properties (fractional anisotropy(FA), axial diffusivity(AD), and radial diffusivity(RD)) of 18 white matter tracts and a general linear model was used to analyze group differences at each age.

Results: Adjusting gestational age at birth, postnatal age at MRI, gender, MRI scanner type, and maternal education, neonates at high risk had significantly lower FA ($p=0.02$) and AD ($p=0.03$) in the superior segment of the left cingulate, and higher RD in the hippocampal segment of the left cingulate ($p=0.04$). High risk one year olds had significantly lower FA ($p<0.01$) and AD ($p=0.02$) in the hippocampal segment of the left cingulate. High risk two year olds had significantly lower FA in the left prefrontal cortico-thalamic tract ($p=0.04$) and higher RD in the right uncinate fasciculus ($p=0.04$). None of the tract differences remained significant after correction for multiple comparisons.

Corresponding author: **John H. Gilmore MD**, UNC Department of Psychiatry, CB#7160, Chapel Hill, NC 27599-7160, USA, Phone: 919-445-0209, john_gilmore@med.unc.edu.

Contributors

Author SA reviewed the literature and wrote the first draft of manuscript. EC reviewed the literature and undertook statistical data. VM collected data and analyzed data. MS designed the study. FJ collected data JG designed the study, wrote the protocol and finalized the manuscript. All authors contributed to and have approved the final manuscript.

Conflict of Interest

None.

Conclusions: There is evidence of abnormal white matter development in young children at risk for schizophrenia, especially in the hippocampal segment of left cingulum. These results support the neurodevelopmental theory of schizophrenia and indicate that impaired white matter may be present in early childhood.

Keywords

Schizophrenia; diffusion; infant; while matter

1. Introduction

Schizophrenia is generally considered a neurodevelopmental disorder with a pathophysiology that likely begins long before the onset of clinical symptoms caused by a combination of multiple environmental and genetic factors (Weinberger, 1987; Lieberman and First, 2018). Pre- and perinatal environmental factors significantly increase risk for schizophrenia, including maternal infection, hypoxia and other obstetric complications (Cannon et al., 2002; Laurens et al., 2015). Many of the genes of risk for schizophrenia play a role in multiple processes important for brain development and plasticity (Schizophrenia Working Group of the Psychiatric Genomics, 2014; Network and Pathway Analysis Subgroup of Psychiatric Genomics, 2015). Lastly, children who later develop schizophrenia are more likely than healthy controls to show minor deviations in motor, cognitive, and social development (Hameed and Lewis, 2016; Filatova et al., 2017).

Schizophrenia is associated with white matter abnormalities and diffusion tensor imaging studies have found decreased fractional anisotropy (FA), along with increased diffusivity within prefrontal and temporal lobes as well as within fiber bundles connecting these regions, including the uncinate fasciculus, cingulum bundle and arcuate fasciculus (Kubicki et al., 2002; Sun et al., 2003; Wang et al., 2004; Kubicki et al., 2007; Ellison-Wright and Bullmore, 2009). Reduced FA in white matter also appear to be present at the first episode of psychosis (Kyriakopoulos and Frangou, 2009). Myelination and maturation of white matter occur rapidly over the first 2 years of life, with a more gradual attainment of adult levels thereafter (Mukherjee et al., 2002; Geng et al., 2012; Dean et al., 2015). We hypothesized that the first 2 years of life is a period in which white matter abnormalities associated with schizophrenia risk may emerge. In this study, we compared diffusion tensor properties of white matter in children at risk for schizophrenia after birth and at one and two years of age with healthy controls.

2. Materials and methods

Participants

This study was approved by the biomedical Institutional Review Board of the University of North Carolina at Chapel Hill and is part of the UNC Early Brain Development Study (Knickmeyer et al., 2008; Gilmore et al., 2010b). Pregnant women with schizophrenia or schizoaffective disorder and control mothers without a history of major psychiatric illness or active substance use during pregnancy were recruited between 2003 and 2014 through inpatient and outpatient psychiatric facilities, emails, and obstetric clinics in central North

Carolina. A few mothers with limited substance use were enrolled if they stopped substance use early in pregnancy (usually after learning they were pregnant). Offspring were scanned at approximately 2-weeks of age and at ages 1 and 2 years. Exclusion criteria for high risk and control infants from this analysis were twin gestation, major medical illness or abnormality on MRI other than a minor intracranial hemorrhage which is common in the neonatal period. Additional exclusions for control subjects were parental psychiatric history or a maternal history of psychotropic medication during pregnancy. Mothers with schizophrenia/schizoaffective disorder were given the Structured Clinical Interview for DSM-IV Axis Disorders (SCID) (Willette et al., 2011) and past medical records were reviewed. A final diagnosis was assigned by two board-certified psychiatrists (LFJ, JHG). Control mothers were screened with a modified SCID questionnaire.

MR Image Acquisition

Infants were scanned unsedated during natural sleep. They were fed prior to scanning, swaddled, and fitted with ear protection, and their heads were secured in a vacuum-fixation device. Most MRI data were acquired on a 3T Siemens Allegra head-only scanner (Siemens Medical System), comprising 89% of the neonates, 82% of the 1-y-olds, and 88% of the 2-y-olds in the present study. For earlier Allegra diffusion-weighted imaging (DWI) data, a single-shot echo-planar imaging spin-echo sequence was used with the following parameters: Repetition Time (TR)/ Echo Time (TE) = 5,200/73 ms, slice thickness = 2 mm, and in-plane resolution = 2 × 2 mm^2, with a total of 45 slices for six directions using b value of 1,000 s/mm^2 and 1 baseline image (b value = 0) per sequence, repeated five times total to improve signal-to-noise. For the remaining Allegra DWI data, 42 directions of diffusion sensitization were acquired with a b value of 1,000 s/mm^2 in addition to seven images with no diffusion weighting for reference. The parameters were as follows: TR/TE/Flip angle = 7,680/82/90°, slice thickness = 2 mm, and in-plane resolution = 2 × 2 mm^2, with a total of 60 to 72 slices. The remaining study subjects were scanned using an upgraded Siemens model, the 3T Tim Trio (Siemens Medical System), following the same sequencing parameters as the 42-direction Allegra sequence detailed above. MRI were same at all three points.

Quantitative tractography

A study-specific quality control protocol was applied to all raw DWI data using DTIPrep (www.nitrc.org/projects/dtiprep), which included slice-wise and gradient-wise artifact detection, as well as eddy current and motion correction (Oguz et al., 2014). This automatic quality control was followed by visual checking of all DWIs, resulting in the exclusion of additional gradients containing artifacts not previously detected. The number of excluded gradients through this quality control checking provides a rough estimate of motion and image quality.

Skull and non-brain tissue was masked out using Brain Extraction Tool (BET) (Smith, 2002), followed by manual correction, if necessary. Tensors were estimated using a weighted least-squares algorithm (Goodlett et al., 2009). Using the UNC –Utah National Alliance for Medical Image Computing diffusion tensor imaging (DTI) framework (https://www.nitrc.org/projects/namicdtifiber) (Verde et al., 2014), we created the UNC EBDS

combined neonate and pediatric (0- 2 y) DTI atlas (https://www.nitrc.org/projects/uncebds_neodti), on which a total of 45 fiber tract segments consistent with reference were reconstructed using streamline tractography using 3D Sheer (https://www.slicer.org). We selected the 18 tracts for analysis as they have associations with cognitive development (Girault et al., 2019) or are altered in schizophrenia (Kubicki et al., 2002; Sun et al., 2003; Wang et al., 2004; Kubicki et al., 2007; Ellison-Wright and Bullmore, 2009): bilateral cingulate superior segments; bilateral cingulate hippocampal segments; bilateral arcuate front-temporal fasciculus; bilateral prefronal cortico-thalamic tract; bilateral inferior longitudinal fasciculus; bilateral superior longitudinal fasciculus; bilateral inferior fronto-occipital fasciculus; bilateral uncinate fasciculus; callosal genu and callosal splenium (Geng et al., 2012; Lee et al., 2015). Each subject's image was deformably registered to the atlas. For group analysis, statistical diffusion profiles were generated for AD, RD, and FA at equally spaced points along the length of each fiber tract and sampled in each subject's original DTI space. These fiber profiles were averaged across the full tract to generate average AD, RD and FA values per tract for use in the following analysis.

Statistical analysis

For demographic variables, frequency distributions were calculated for categorical variables, and the means and SDs were calculated for continuous variables. General linear models were used to analyze the differences in the diffusion properties (AD, RD, and FA) between children at high risk for schizophrenia and healthy controls. Least square-means and p-values were calculated for all analyses. Model 1 was adjusted for gestational age at birth, postnatal age at MRI, gender, and MRI scanner type/number of directions. MRI scanner type/number of directions are divided into 3 categories (Allegra 6 directions, Allegra 42 directions, and Trio 42 directions) and regarded as categorical variables in the model. Model 2 was adjusted for Model 1 covariates as well as maternal education. Model 3 was adjusted for Model 2 covariates as well as paternal age. Adjustment for multiple comparisons was also performed using the Benjamini-Hochberg false discovery rate (FDR) procedure (Benjamini et al., 2001). Statistical significance level was set at an alpha level of 0.05. All analyses were done with SAS, version 9.4 (SAS Institute, Cary, U.S.A), using GLM procedure.

3. Results

Tract-averaged DTI metric data were extracted for 312 subjects (269 healthy control, 43 high risk). In high risk and healthy controls, eight subjects were excluded because they were twins and eight subjects had major medical illness or brain abnormality on MRI. In healthy controls, 56 subjects were excluded for a maternal history of taking psychotropic medications. A total of 240 subjects (202 healthy control, 38 high risk) were included in this study: 161 subjects (143 healthy control, 18 high risk) at neonate, 119 subjects (92 healthy control, 27 high risk) at one year, and 92 subjects (70 healthy control, 22 high risk) at two year with DTI metric data

Table 1 summarizes the sociodemographic variables for the healthy controls and high-risk groups. Gestational age at birth, birth weight, maternal age at birth, maternal education,

maternal ethnicity, drug use and age at neonatal and two year scan were significantly different between two groups ($p<0.05$).

Table 2 provides the average number of gradients excluded during both quality control steps. Images obtained using 6 directions could retain a maximum of 30 gradients, and 42-direction images could retain as many as 42 gradients. There were no significant differences in the number of excluded gradients between the high risk and control groups at any age or from any scanner/sequence type.

Model 1 tract average FA, AD, and RD values for the 18 white matter tracts studied are presented in Tables 3, 4 and 5. DTI properties of seven tracts of high risk are significantly different from those of healthy controls (Fig.1). Neonates at high risk for schizophrenia had significantly lower FA in the superior segment of the left cingulate ($p=0.03$) and the right uncinate fasciculus ($p=0.03$). RD was significantly higher in the hippocampal segment of the left cingulate ($p<0.01$) compared to healthy controls. There were no significant differences in AD. High risk one year olds had significantly reduced FA in the left fronto-temporal arcuate fasciculus ($p=0.03$), hippocampal segment of the left cingulate ($p<0.01$) and significant lower AD in the hippocampal segment of the left cingulate ($p=0.02$). There were no significant differences in RD. High risk two year olds had significantly lower FA in the left frontotemporal arcuate fasciculus ($p=0.03$), hippocampal segment of the left cingulate ($p=0.01$), left prefrontal cortico-thalamic tract ($p<0.01$) and bilateral superior longitudinal fasciculus ($p=0.04$). RD was significantly higher in the bilateral superior longitudinal fasciculus ($p=0.02$ for left side and $p=0.03$ for right side) compared to controls. There were no differences in AD. To better understand the contribution of the differences in maternal education in the high risk and control groups, we performed similar analyses adding a maternal education as a covariate (Model 2) and maternal education and paternal age as covariates (Model 3). In Model 2, several white matter tracts remained significant after controlling for maternal education (Table 6, Supplemental Table 1,2,3). These include lower FA and AD in the superior segment of the left cingulate ($p=0.02$ and $p=0.03$ respectively) and higher RD in the hippocampal segment of the left cingulate ($p=0.04$) of high risk neonates, lower FA and AD in the hippocampal segment of the left cingulate ($p<0.01$ and $p=0.02$ respectively) of high risk one year olds, and lower FA in the left prefrontal cortico-thalamic tract ($p=0.04$) and higher RD in right uncinate fasciculus ($p=0.04$) of high risk 2 year olds. None of the tract differences remained significant after correction for multiple comparisons. In a final model (Model 3), we explored the contribution of paternal age to the findings, and many white matter tracts remained significant (Supplemental Table 4,5,6).

4. Discussion

In this study, we tested the hypothesis that abnormal white matter microstructure associated with risk for schizophrenia can be detected in the first 2 years of life. Overall, we found few differences, though interestingly, RD was significantly higher in the hippocampal segment of the left cingulum in the high risk group at birth. FA values were significantly lower in this tract at ages 1 and 2 years. AD was also significantly lower at age one. In addition, high risk children had some differences of diffusion properties in the superior segment of the left cingulum and the right uncinate fasciculus after birth, and in the left fronto-temporal arcuate

fasciculus, the left prefronal cortico-thalamic tract, and bilateral superior longitudinal fasciculus in one and 2 year olds. This suggests that, within the limits of this study, there may be microstructure differences in infants at high risk for schizophrenia that deserve further study.

We previously studied diffusion properties in the corpus callosum and cortico-spinal tracts in neonates at high risk for schizophrenia with those of healthy controls and found no differences (Gilmore et al., 2010a). The most notable finding in the current study was that diffusion properties in the left cingulum hippocampal segment in high risk were consistently abnormal at each age (higher RD at birth, lower FA and AD at 1 year and lower FA at 2 year). The cingulum bundle is a white matter tract that underlies the cingulate cortex, connecting the cingulate cortex with multiple brain regions, including premotor and prefrontal regions, thalamus, parahippocampal gyrus, and other cortical association regions (Jones et al., 2013). Previous studies have observed FA abnormalities in adults with schizophrenia in the cingulum (Wang et al., 2004; Fujiwara et al., 2007), and symptoms of schizophrenia have been associated with these connections; dysfunction of cingulum has been proposed as a core feature of schizophrenia (Jones et al., 2006; Anticevic and Corlett, 2012). A voxel based analysis found that lower FA at right anterior cingulum bundle in first-episode schizophrenia (Hao et al., 2006). Another study also reported that adolescents with early-onset schizophrenia demonstrated a significantly reduced FA in the right anterior cingulum bundle, which may reflect core pathophysiological disturbances rather than chronic structural changes (Tang et al., 2010). FA represents shape of diffusion ellipsoid and is highly sensitive to the microstructural integrity of fibers (Acosta-Cabronero et al., 2010). AD represents the microscopic water movement parallel to the axonal tracts and is linked with axonal damage (Budde et al., 2009). RD represents the microscopic water movement perpendicular to axonal tracts and is linked with myelin damage (Tae et al., 2018). A previous study demonstrated that myelinated fiber of cingulum is observed in healthy infant at birth (Welker and Patton, 2012). From this perspective, the higher RD in high risk at birth in our study may represent delayed myelination of cingulum which may affect the white matter integrity of 1 year and 2 year. However, caution should be taken with the interpretation of DTI metrics as they are sensitive to various developmental events including pre-myelination, myelination, and myelination of crossing fiber (Pierpaoli et al., 2001; Girault et al., 2019).

We also found that the left front temporal arcuate fasciculus showed reduced FA at age 1 and 2 years; left prefrontal cortico-thalamic tract and bilateral superior longitudinal fasciculus also demonstrated reduced FA at age 2 years. The left fronto temporal arcuate fasciculus connects language related regions such as Wernicke’s area with the frontal cortex and may underlie language anomalies and auditory hallucinations found in schizophrenia (Catani et al., 2005; Psomiades et al., 2016). Dysfunction of the cortico-thalamic tract is thought to contribute to fundamental cognitive deficit in schizophrenia (Kubota et al., 2013) and abnormalities of pathways to prefrontal regions is thought to constitute a putative pathology (Volk and Lewis, 2010). Structural studies have shown frontal and parietal gray matter atrophy in early stage of schizophrenia (Narr et al., 2005; Whitford et al., 2006) and recent-onset schizophrenia patients show deficits in superior longitudinal fasiculus, the major connection between prefrontal and parietal cortices (Karlsgodt et al., 2008). Geng et al

investigated 211 healthy children from birth to two years using DTI analysis, and found that arcuate fasciculus showed lower degree of maturation at birth, but relatively faster maturation rate in the first two year, which might explain a delayed abnormality of this tract in our result (Geng et al., 2012). It could also be interpreted to mean that each individual white matter tract may become altered during different periods of development. However, regarding arcuate fasciculus, cortico thalamic tract and superior longitudinal fasciculus, further follow-up with children older than two years is necessary to confirm our results.

In our analysis, the addition of maternal education as a covariate eliminated the significance of some white matter tracts, suggesting that maternal education may affect white matter microstructure associated with schizophrenia in early childhood. People with schizophrenia are more likely to reside in areas with higher social deprivation and have lower socioeconomic status (Dohrenwend, 1990; Byrne et al., 2004). The difference in socioeconomic status between the groups, reflected in maternal education, may contribute to our findings independent of risk status, as here is a rich literature describing the association between maternal education and early brain development. (Bornstein and Bradley, 2014; Rochette and Bernier, 2014). However, it is also quite possible that controlling for maternal education removes true associations between risk status and diffusion properties as cognitive impairment and less educational attainment is a common feature of schizophrenia. Higher paternal age is associated with increased risk of schizophrenia in the offspring (Wohl and Gorwood, 2007; Torrey et al., 2009; Miller et al., 2011), perhaps due to an increase in the rate of de novo genetic mutation in older fathers. In our study, paternal age did not appear to impact the results.

DTI signals can be affected by various factors including field strength, scanner manufacture, gradient strength/directions, and b-value (Magnotta et al., 2012). Pagani et al found a significant influence of magnetic field strength and scanner manufacturer on MD and AD measures (Pagani et al., 2010). Pfefferbaum et al showed that different gradient strength resulted in a 2% difference in FA values (Pfefferbaum et al., 2003). Johns et al found that 20 directions were required to get a robust estimation of FA value and 30 directions were required for MD. We used two different types of scanners with same magnetic field strength (3T), and similar gradient strength (40~45 mT/m). The different scanners and directions used in this study is a limitation that we addressed by regressing out scanner type and number of gradient directions. Head motion during scan is also a potential confounder, as head motion can result in misalignment of diffusion images and attenuated image intensity. Signal attenuation due to macroscopic head motion can confound microscopic random motion of water molecules in tissues (Yendiki et al., 2014). Makowski et al. suggested prospective and retrospective procedures for correction of head motion (Makowski et al., 2018). To address this issue, we excluded gradient with head motion during preprocessing step. Importantly, the number of excluded images due to head motion was not significantly different between the high risk and control groups in our study.

This study has other limitations. First, this study has an unbalanced sample size; with a relatively small high risk group and a larger control group. Second, our high risk group was composed of offspring of mothers with schizophrenia or schizoaffective disorder; this heterogeneity should be considered when interpreting results. Finally, it is difficult to

separate the effects of genetic risk from the environmental risks associated with having a mother with schizophrenia (i.e. sub-optimal prenatal course and infant environment). Whatever the ultimate causative factors turn out to be, our study does suggest that having a mother with schizophrenia influences white matter maturation in white matter tracts important for schizophrenia. Our initial findings may serve as a cornerstone for future studies with a larger sample to validate and extend these results.

In summary, infants at risk for schizophrenia showed evidence of abnormal white matter integrities in some white matter tracts implicated in studies of adults with schizophrenia. These results suggest that early white matter development is altered in infants at risk for schizophrenia and support the neurodevelopmental theory of schizophrenia.

Supplementary Material

Refer to Web version on PubMed Central for supplementary material.

Acknowledgement

Source of funding

Supported by NIH grants MH064065 and HD053000 to JHG.

References

Acosta-Cabronero J, Williams GB, Pengas G, Nestor PJ, 2010 Absolute diffusivities define the landscape of white matter degeneration in Alzheimer's disease. Brain 133 (Pt 2), 529–539. [PubMed: 19914928]

Anticevic A, Corlett PR, 2012 Cognition–emotion dysinteraction in schizophrenia. Front Psychol 3, 392. [PubMed: 23091464]

Benjamini Y, Drai D, Elmer G, Kafkafi N, Golani I, 2001 Controlling the false discovery rate in behavior genetics research. Behav Brain Res 125 (1-2), 279–284. [PubMed: 11682119]

Bornstein MH, Bradley RH, 2014 Socioeconomic status, parenting, and child development. Routledge.

Budde MD, Xie M, Cross AH, Song SK, 2009 Axial diffusivity is the primary correlate of axonal injury in the experimental autoimmune encephalomyelitis spinal cord: a quantitative pixelwise analysis. J Neurosci 29 (9), 2805–2813. [PubMed: 19261876]

Byrne M, Agerbo E, Eaton WW, Mortensen PB, 2004 Parental socio-economic status and risk of first admission with schizophrenia– a Danish national register based study. Soc Psychiatry Psychiatr Epidemiol 39 (2), 87–96. [PubMed: 15052389]

Cannon M, Jones PB, Murray RM, 2002 Obstetric complications and schizophrenia: historical and meta-analytic review. Am J Psychiatry 159 (7), 1080–1092. [PubMed: 12091183]

Catani M, Jones DK, ffytche DH, 2005 Perisylvian language networks of the human brain. Ann Neurol 57 (1), 8–16. [PubMed: 15597383]

Dean DC 3rd, O'Muircheartaigh J, Dirks H, Waskiewicz N, Walker L, Doernberg E, Piryatinsky I, Deoni SC, 2015 Characterizing longitudinal white matter development during early childhood. Brain Struct Funct 220 (4), 1921–1933. [PubMed: 24710623]

Dohrenwend BP, 1990 Socioeconomic status (SES) and psychiatric disorders. Are the issues still compelling? Soc Psychiatry Psychiatr Epidemiol 25 (1), 41–47. [PubMed: 2406949]

Ellison-Wright I, Bullmore E, 2009 Meta-analysis of diffusion tensor imaging studies in schizophrenia. Schizophr Res 108 (1-3), 3–10. [PubMed: 19128945]

Filatova S, Koivumaa-Honkanen H, Hirvonen N, Freeman A, Ivandic I, Hurtig T, Khandaker GM, Jones PB, Moilanen K, Miettunen J, 2017 Early motor developmental milestones and

schizophrenia: A systematic review and meta-analysis. Schizophr Res 188, 13–20. [PubMed: 28131598]

Fujiwara H, Namiki C, Hirao K, Miyata J, Shimizu M, Fukuyama H, Sawamoto N, Hayashi T, Murai T, 2007 Anterior and posterior cingulum abnormalities and their association with psychopathology in schizophrenia: a diffusion tensor imaging study. Schizophr Res 95 (1-3), 215–222. [PubMed: 17664062]

Geng X, Gouttard S, Sharma A, Gu H, Styner M, Lin W, Gerig G, Gilmore JH, 2012 Quantitative tract-based white matter development from birth to age 2years. Neuroimage 61 (3), 542–557. [PubMed: 22510254]

Gilmore JH, Kang C, Evans DD, Wolfe HM, Smith JK, Lieberman JA, Lin W, Hamer RM, Styner M, Gerig G, 2010a Prenatal and neonatal brain structure and white matter maturation in children at high risk for schizophrenia. Am J Psychiatry 167 (9), 1083–1091. [PubMed: 20516153]

Gilmore JH, Schmitt JE, Knickmeyer RC, Smith JK, Lin W, Styner M, Gerig G, Neale MC, 2010b Genetic and environmental contributions to neonatal brain structure: A twin study. Hum Brain Mapp 31 (8), 1174–1182. [PubMed: 20063301]

Girault JB, Cornea E, Goldman BD, Knickmeyer RC, Styner M, Gilmore JH, 2019 White matter microstructural development and cognitive ability in the first 2 years of life. Hum Brain Mapp 40 (4), 1195–1210. [PubMed: 30353962]

Goodlett CB, Fletcher PT, Gilmore JH, Gerig G, 2009 Group analysis of DTI fiber tract statistics with application to neurodevelopment. Neuroimage 45 (1 Suppl), S133–142. [PubMed: 19059345]

Hameed MA, Lewis AJ, 2016 Offspring of Parents with Schizophrenia: A Systematic Review of Developmental Features Across Childhood. Harv Rev Psychiatry 24 (2), 104–117. [PubMed: 26954595]

Hao Y, Liu Z, Jiang T, Gong G, Liu H, Tan L, Kuang F, Xu L, Yi Y, Zhang Z, 2006 White matter integrity of the whole brain is disrupted in first-episode schizophrenia. Neuroreport 17 (1), 23–26. [PubMed: 16361944]

Jones DK, Catani M, Pierpaoli C, Reeves SJ, Shergill SS, O'Sullivan M, Golesworthy P, McGuire P, Horsfield MA, Simmons A, Williams SC, Howard RJ, 2006 Age effects on diffusion tensor magnetic resonance imaging tractography measures of frontal cortex connections in schizophrenia. Hum Brain Mapp 27 (3), 230–238. [PubMed: 16082656]

Jones DK, Christiansen KF, Chapman RJ, Aggleton JP, 2013 Distinct subdivisions of the cingulum bundle revealed by diffusion MRI fibre tracking: implications for neuropsychological investigations. Neuropsychologia 51 (1), 67–78. [PubMed: 23178227]

Karlsgodt KH, van Erp TG, Poldrack RA, Bearden CE, Nuechterlein KH, Cannon TD, 2008 Diffusion tensor imaging of the superior longitudinal fasciculus and working memory in recent-onset schizophrenia. Biol Psychiatry 63 (5), 512–518. [PubMed: 17720147]

Knickmeyer RC, Gouttard S, Kang C, Evans D, Wilber K, Smith JK, Hamer RM, Lin W, Gerig G, Gilmore JH, 2008 A structural MRI study of human brain development from birth to 2 years. J Neurosci 28 (47), 12176–12182. [PubMed: 19020011]

Kubicki M, McCarley R, Westin CF, Park HJ, Maier S, Kikinis R, Jolesz FA, Shenton ME, 2007 A review of diffusion tensor imaging studies in schizophrenia. J Psychiatr Res 41 (1-2), 15–30. [PubMed: 16023676]

Kubicki M, Westin CF, Maier SE, Frumin M, Nestor PG, Salisbury DF, Kikinis R, Jolesz FA, McCarley RW, Shenton ME, 2002 Uncinate fasciculus findings in schizophrenia: a magnetic resonance diffusion tensor imaging study. Am J Psychiatry 159 (5), 813–820. [PubMed: 11986136]

Kubota M, Miyata J, Sasamoto A, Sugihara G, Yoshida H, Kawada R, Fujimoto S, Tanaka Y, Sawamoto N, Fukuyama H, Takahashi H, Murai T, 2013 Thalamocortical disconnection in the orbitofrontal region associated with cortical thinning in schizophrenia. JAMA Psychiatry 70 (1), 12–21. [PubMed: 22945538]

Kyriakopoulos M, Frangou S, 2009 Recent diffusion tensor imaging findings in early stages of schizophrenia. Curr Opin Psychiatry 22 (2), 168–176. [PubMed: 19553871]

Laurens KR, Luo L, Matheson SL, Carr VJ, Raudino A, Harris F, Green MJ, 2015 Common or distinct pathways to psychosis? A systematic review of evidence from prospective studies for

developmental risk factors and antecedents of the schizophrenia spectrum disorders and affective psychoses. BMC Psychiatry 15, 205. [PubMed: 26302744]

Lee SJ, Steiner RJ, Luo S, Neale MC, Styner M, Zhu H, Gilmore JH, 2015 Quantitative tract-based white matter heritability in twin neonates. Neuroimage 111, 123–135. [PubMed: 25700954]

Lieberman JA, First MB, 2018 Psychotic Disorders. N Engl J Med 379 (3), 270–280. [PubMed: 30021088]

Magnotta VA, Matsui JT, Liu D, Johnson HJ, Long JD, Bolster BD Jr., Mueller BA, Lim K, Mori S, Helmer KG, Turner JA, Reading S, Lowe MJ, Aylward E, Flashman LA, Bonett G, Paulsen JS, 2012 Multicenter reliability of diffusion tensor imaging. Brain Connect 2 (6), 345–355. [PubMed: 23075313]

Makowski C, Lepage M, Evans AC, 2018 Head motion: the dirty little secret of neuroimaging in psychiatry. J Psychiatry Neurosci 43 (5), 180022. [PubMed: 30106360]

Miller B, Suvisaari J, Miettunen J, Jarvelin M-R, Haukka J, Tanskanen A, Lonnqvist J, Isohanni M, Kirkpatrick B, 2011 Advanced paternal age and parental history of schizophrenia. Schizophrenia research 133 (1-3), 125–132. [PubMed: 21937198]

Mukherjee P, Miller JH, Shimony JS, Philip JV, Nehra D, Snyder AZ, Conturo TE, Neil JJ, McKinstry RC, 2002 Diffusion-tensor MR imaging of gray and white matter development during normal human brain maturation. AJNR Am J Neuroradiol 23 (9), 1445–1456. [PubMed: 12372731]

Narr KL, Bilder RM, Toga AW, Woods RP, Rex DE, Szeszko PR, Robinson D, Sevy S, Gunduz-Bruce H, Wang YP, DeLuca H, Thompson PM, 2005 Mapping cortical thickness and gray matter concentration in first episode schizophrenia. Cereb Cortex 15 (6), 708–719. [PubMed: 15371291]

Network, Pathway Analysis Subgroup of Psychiatric Genomics, C., 2015 Psychiatric genome-wide association study analyses implicate neuronal, immune and histone pathways. Nat Neurosci 18 (2), 199–209. [PubMed: 25599223]

Pagani E, Hirsch JG, Pouwels PJ, Horsfield MA, Perego E, Gass A, Roosendaal SD, Barkhof F, Agosta F, Rovaris M, Caputo D, Giorgio A, Palace J, Marino S, De Stefano N, Ropele S, Fazekas F, Filippi M, 2010 Intercenter differences in diffusion tensor MRI acquisition. J Magn Reson Imaging 31 (6), 1458–1468. [PubMed: 20512899]

Pfefferbaum A, Adalsteinsson E, Sullivan EV, 2003 Replicability of diffusion tensor imaging measurements of fractional anisotropy and trace in brain. J Magn Reson Imaging 18 (4), 427–433. [PubMed: 14508779]

Pierpaoli C, Barnett A, Pajevic S, Chen R, Penix ER, Virta A, Basser P, 2001 Water diffusion changes in Wallerian degeneration and their dependence on white matter architecture. Neuroimage 13 (6 Pt 1), 1174–1185. [PubMed: 11352623]

Psomiades M, Fonteneau C, Mondino M, Fuck D, Haesebaert F, Suaud-Chagny MF, Brunelin J, 2016 Integrity of the arcuate fasciculus in patients with schizophrenia with auditory verbal hallucinations: A DTI-tractography study. Neuroimage Clin 12, 970–975. [PubMed: 27995063]

Rochette É, Bernier A, 2014 Parenting, family socioeconomic status, and child executive functioning: A longitudinal study. Merrill-Palmer Quarterly (1982–) 60 (4), 431–460.

Schizophrenia Working Group of the Psychiatric Genomics, C., 2014 Biological insights from 108 schizophrenia-associated genetic loci. Nature 511 (7510), 421–427. [PubMed: 25056061]

Smith SM, 2002 Fast robust automated brain extraction. Hum Brain Mapp 17 (3), 143–155. [PubMed: 12391568]

Sun Z, Wang F, Cui L, Breeze J, Du X, Wang X, Cong Z, Zhang H, Fi B, Hong N, Zhang D, 2003 Abnormal anterior cingulum in patients with schizophrenia: a diffusion tensor imaging study. Neuroreport 14 (14), 1833–1836. [PubMed: 14534430]

Tae WS, Ham BJ, Pyun SB, Kang SH, Kim BJ, 2018 Current Clinical Applications of Diffusion-Tensor Imaging in Neurological Disorders. J Clin Neurol 14 (2), 129–140. [PubMed: 29504292]

Tang J, Fiao Y, Zhou B, Tan C, Fiu T, Hao W, Hu D, Chen X, 2010 Abnormal anterior cingulum integrity in first episode, early-onset schizophrenia: a diffusion tensor imaging study. Brain Res 1343, 199–205. [PubMed: 20452334]

Torrey EF, Buka S, Cannon TD, Goldstein JM, Seidman FJ, Fiu T, Hadley T, Rosso IM, Bearden C, Yolken RH, 2009 Paternal age as a risk factor for schizophrenia: how important is it? Schizophrenia research 114 (1-3), 1–5. [PubMed: 19683417]

Verde AR, Budin F, Berger JB, Gupta A, Farzinfar M, Kaiser A, Ahn M, Johnson H, Matsui J, Hazlett HC, Sharma A, Goodlett C, Shi Y, Gouttard S, Vachet C, Piven J, Zhu H, Gerig G, Styner M, 2014 UNC–Utah NA–MIC framework for DTI fiber tract analysis. Front Neuroinform 7, 51. [PubMed: 24409141]

Volk DW, Lewis DA, 2010 Prefrontal cortical circuits in schizophrenia. Curr Top Behav Neurosci 4, 485–508. [PubMed: 21312410]

Wang F, Sun Z, Cui L, Du X, Wang X, Zhang H, Cong Z, Hong N, Zhang D, 2004 Anterior cingulum abnormalities in male patients with schizophrenia determined through diffusion tensor imaging. Am J Psychiatry 161 (3), 573–575. [PubMed: 14992988]

Weinberger DR, 1987 Implications of normal brain development for the pathogenesis of schizophrenia. Arch Gen Psychiatry 44 (7), 660–669. [PubMed: 3606332]

Welker KM, Patton A, 2012 Assessment of normal myelination with magnetic resonance imaging. Semin Neurol 32 (1), 15–28. [PubMed: 22422203]

Whitford TJ, Grieve SM, Farrow TF, Gomes L, Brennan J, Harris AW, Gordon E, Williams LM, 2006 Progressive grey matter atrophy over the first 2–3 years of illness in first-episode schizophrenia: a tensor-based morphometry study. Neuroimage 32 (2), 511–519. [PubMed: 16677830]

Willette AA, Lubach GR, Knickmeyer RC, Short SJ, Styner M, Gilmore JH, Coe CL, 2011 Brain enlargement and increased behavioral and cytokine reactivity in infant monkeys following acute prenatal endotoxemia. Behav Brain Res 219 (1), 108–115. [PubMed: 21192986]

Wohl M, Gorwood P, 2007 Paternal ages below or above 35 years old are associated with a different risk of schizophrenia in the offspring. European Psychiatry 22 (1), 22–26. [PubMed: 17142012]

Yendiki A, Koldewyn K, Kakunoori S, Kanwisher N, Fischl B, 2014 Spurious group differences due to head motion in a diffusion MRI study. Neuroimage 88, 79–90. [PubMed: 24269273]

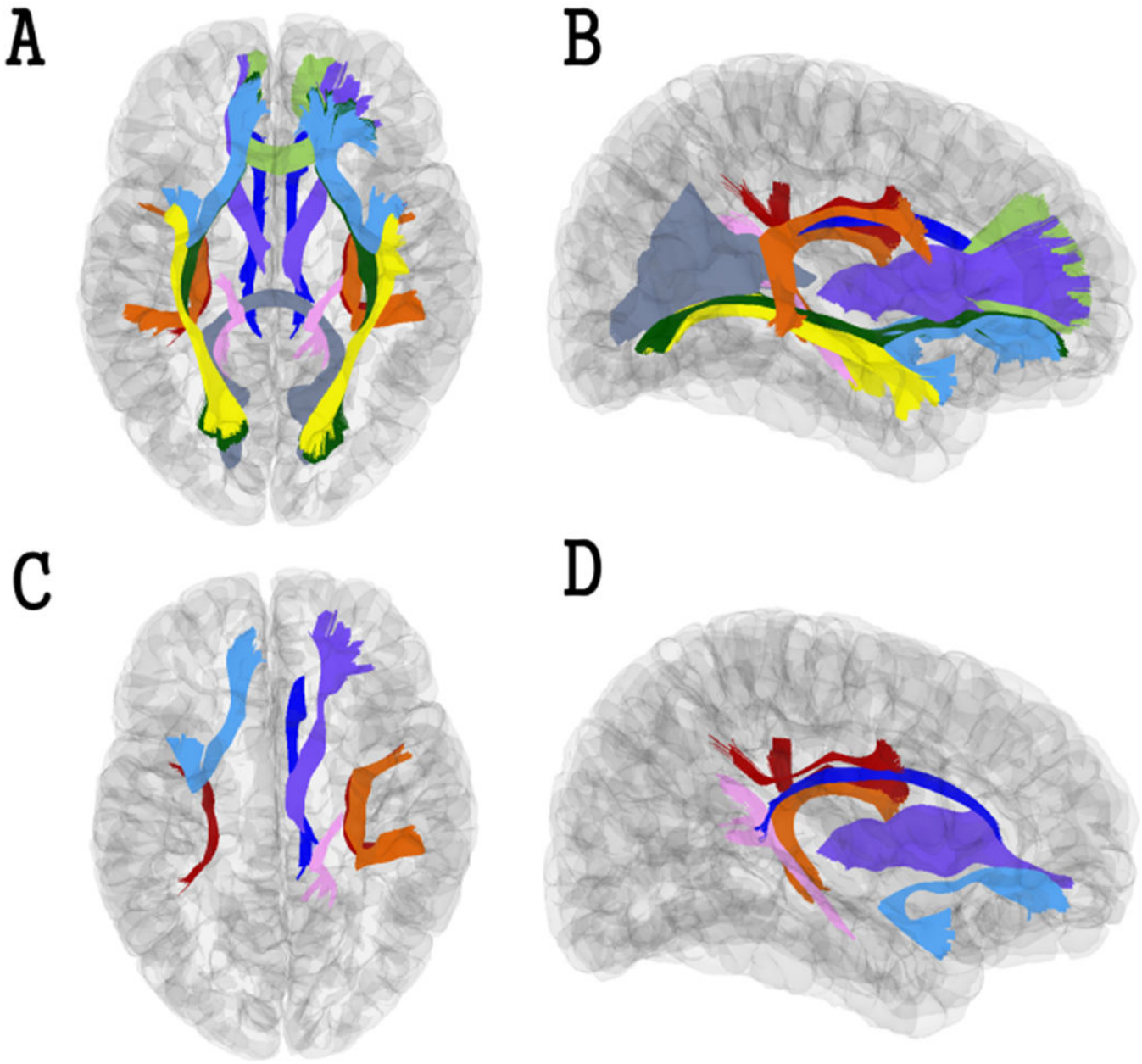

Fig 1.

18 white matter tracts which are associated with cognitive development or known to be altered in schizophrenia (A,B). Seven significant tracts in which DTI properties of high risk are different from those of healthy controls in model 1 (C,D). Bilateral cingulate superior segments = dark blue; bilateral cingulate hippocampal segments=pink; bilateral arcuate fronto-temporal fasciculus=orange; bilateral prefrontal cortico-thalamic tract=purple; bilateral inferior longitudinal fasciculus=yellow; bilateral superior longitudinal fasciculus=red; bilateral inferior fronto-occipital fasciculus=dark green; bilateral uncinate fasciculus=light; blue genu=light green; splenium=gray.

Table 1.

Demographic characteristics of children at high risk for schizophrenia and healthy controls.

Demographics	Healthy control (n=202)	High risk for schizophrenia (n=38)	P-value
Number of subjects (Neonates/1 Year/2 Year)	143/92/70	18/27/22	
Gestational Age at Birth (Days)	275.6 ± 10.98	267.1 ± 15.80	<0.01*
Birth Weight (grams)	3387 ± 487.0	3022 ± 686.5	<0.01*
Gender (female)	97 (48.02)	19 (50.0)	0.86
Maternal Age at Child Birth (Years)	30.15 ± 5.05	26.73 ± 6.18	<0.01*
Paternal Age at Child Birth (Years)	31.85 ± 5.27	35.63 ± 13.03	<0.54
Maternal Education (Years)	16.20 ± 3.10	9.81 ± 3.11	<0.01*
Paternal Education (Years)	16.07 ±3.33	10.30 ±3.28	<0.01*
Mother Ethnicity	165/33/4 (81.68/16.34/1.98)	10/27/1 (26.32/71.05/2.63)	<0.01*
White/African American/Asian			
Drag use (yes/no)	0/202 (0/100)	4/34 (10.53/89.47)	<0.01*
Age at MRI (Days)			
Neonates	22.52 ± 11.41	32.68 ± 16.31	0.01*
1 Year	382.9 ± 22.61	390.3 ± 31.71	0.68
2 Year	745.3 ± 25.01	766.8 ± 42.00	0.03*
Scanner Direction A6 /A42/T42			
Neonates	86/39/18(60.14/27.27/12.59)	9/8/1(50.00/44.44/5.56)	0.02*
1 Year	31/44/17(33.70/47.83/18.48)	12/13/2(44.44/48.15/7.41)	0.02*
2 Year	27/35/8(38.57/50.00/11.43)	9/9/4(40.91/40.91/18.18)	0.04*

Continuous variables represent mean ± standard deviation; categorical variables represent number (percentage)

* $p < 0.05$

Table 2.

Summary of gradients excluded during automatic and visual quality control

	Neonate			1 Year			2 Year		
	Control ***M (SD)***	**High Risk** ***M (SD)***	***p***	**Control** ***M (SD)***	**High Risk** ***M (SD)***	***p***	**Control** ***M (SD)***	**High Risk** ***M (SD)***	***p***
Allegra, 6-direction	4.65 (3.94)	3.00 (3.35)	0.229	1.26 (2.76)	1.67 (3.23)	0.680	1.93 (3.66)	1.89 (4.26)	0.980
Allegra, 42-direction	5.54 (4.99)	4.63 (4.17)	0.632	4.09 (3.52)	4.46 (3.31)	0.737	4.34 (4.68)	3.78 (1.86)	0.726
Trio, 42-direction	3.56 (4.87)	2.00 (.)	0.759	5.82 (4.67)	11.00 (2.83)	0.149	5.25 (2.92)	4.25 (4.19)	0.637

Note. For the 6-direction scans, the maximum number of gradients remaining is 30. For the 42-direction scans, the maximum number of gradients remaining is 42. *M* refers to the average number of gradients excluded during quality control, *p* refers to the *p*-value of the *T*-test comparing the number of gradients excluded between control and high risk groups.

Table 3.

Comparison of least square means of DTI metrics of 18 white matter tract between neonate at risk for schizophrenia and healthy controls. The model 1 was adjusted by gestational age at birth, gender, postnatal age at MRI, and MRI scanner type

	FA			AD			RD		
Tract	**LSM(SE) HC**	**LSM(SE)HR**	**P value**	**LSM(SE) HC**	**LSM(SE)HR**	**P value**	**LSM(SE) HC**	**LSM(SE)HR**	**P value**
Arc_FT_L	0.1752 (0.00132)	0.1720 (0.00338)	0.36	0.0015 (0.00001)	0.0015 (0.00002)	0.86	0.0012 (0.00001)	0.0012 (0.00001)	0.43
Arc_FT_R	0.1983 (0.00143)	0.1964 (0.00359)	0.62	0.0015 (0.00001)	0.0016 (0.00001)	0.63	0.0012 (0.00001)	0.0012 (0.00001)	0.46
Cing_G_L	0.1792 (0.00173)	0.1692 (0.00440)	0.03 *	0.0015 (0.00001)	0.0015 (0.00002)	0.20	0.0011 (0.00000)	0.0011 (0.00001)	0.99
Cing_G_R	0.1753 (0.00181)	0.1718 (0.00457)	0.47	0.0015 (0.00001)	0.0015 (0.00002)	0.97	0.0012 (0.00001)	0.0012 (0.00001)	0.58
Cing_H_L	0.1759 (0.00173)	0.1655 (0.00498)	0.05	0.0015 (0.00000)	0.0015 (0.00001)	0.13	0.0011 (0.00000)	0.0012 (0.00001)	<0.01 **
Cing_H_R	0.1718 (0.00168)	0.1716 (0.00419)	0.96	0.0015 (0.00000)	0.0015 (0.00001)	0.67	0.0011 (0.00000)	0.0011 (0.00001)	0.74
CT_PreF_L	0.1887 (0.00121)	0.1867 (0.00309)	0.53	0.0015 (0.00001)	0.0015 (0.00001)	0.23	0.0011 (0.00001)	0.0011 (0.00001)	0.27
CT_PreF_R	0.1904 (0.00126)	0.1851 (0.00323)	0.11	0.0015 (0.00001)	0.0015 (0.00001)	0.42	0.0011 (0.00001)	0.0011 (0.00001)	0.13
ILF_L	0.2328 (0.00176)	0.2260 (0.00449)	0.14	0.0017 (0.00001)	0.0017 (0.00002)	0.95	0.0012 (0.00001)	0.0012 (0.00001)	0.41
ILF_R	0.2278 (0.00169)	0.2220 (0.00432)	0.19	0.0016 (0.00001)	0.0016 (0.00002)	0.81	0.0011 (0.00000)	0.0012 (0.00001)	0.31
SLF_L	0.1621 (0.00150)	0.1614 (0.00382)	0.85	0.0015 (0.00001)	0.0015 (0.00001)	0.74	0.0011 (0.00001)	0.0011 (0.00001)	0.72
SLF_R	0.1639 (0.00141)	0.1614 (0.00367)	0.51	0.0015 (0.00001)	0.0014 (0.00001)	0.52	0.0011 (0.00001)	0.0011 (0.00001)	0.69
IFOF_L	0.2355 (0.00152)	0.2311 (0.00390)	0.27	0.0016 (0.00001)	0.0016 (0.00002)	0.32	0.0011 (0.00001)	0.0012 (0.00001)	0.20
IFOF_R	0.2304 (0.00146)	0.2255 (0.00375)	0.20	0.0016 (0.00001)	0.0016 (0.00002)	0.51	0.0011 (0.00001)	0.0012 (0.00001)	0.28
UNC_L	0.1919 (0.00134)	0.1880 (0.00343)	0.27	0.0015 (0.00001)	0.0015 (0.00001)	0.23	0.0011 (0.00001)	0.0012 (0.00001)	0.16
UNC_R	0.2003 (0.00139)	0.1925 (0.00356)	0.03 *	0.0015 (0.00001)	0.0016 (0.00001)	0.25	0.0011 (0.00001)	0.0012 (0.00001)	0.10
CC_Genu	0.2541 (0.00198)	0.2455 (0.00508)	0.10	0.0017 (0.00001)	0.0018 (0.00002)	0.35	0.0012 (0.00001)	0.0012 (0.00002)	0.13
CC_Splen	0.2773 (0.00205)	0.2782 (0.00526)	0.87	0.0017 (0.00001)	0.0017 (0.00002)	0.15	0.0011 (0.00001)	0.0011 (0.00001)	0.47

FA, fractional anisotropy; AD, axial diffusivity; RD, radial diffusivity; LSM, least square mean; SE, standard error

Arc_FT_L, left arcuate front-temporal fasciculus; Arc_FT_R, right arcuate front-temporal fasciculus; Cing_G_L, left cingulate superior segment; Cing_G_R, right cingulate superior segment; Cing_H_L, left cingulate hippocampal segment; Cing_H_R, right cingulate hippocampal segment; CT_PreF_L, left prefronal corticothalamic tract; CT_PreF_R, right prefronal cortico-thalamic tract; ILF_L, left inferior longitudinal fasciculus; ILF_R, right inferior longitudinal fasciculus; SLF_L, left superior longitudinal fasciculus; SLF_R, right superior longitudinal fasciculus; IFOF_L, left inferior fronto-occipital fasciculus; IFOF_R, right inferior fronto-occipital fasciculus; UNC_L, left uncinated fasciculus; UNC_R, right uncinated fasciculus; CC_Genu, callosal genu; CC_Splen, callosal splenium

* $p < 0.05$;

** $p < 0.01$;

† $p < 0.05$ after FDR correction

Table 4.

Comparison of least square means of DTI metrics of 18 white matter tract between one year olds at risk for schizophrenia and healthy control. Model 1 was adjusted by gestational age at birth, gender, postnatal age at MRI, and MRI scanner type

	FA			AD			RD		
Tract	**LSM(SE) HC**	**LSM(SE)HR**	**P value**	**LSM(SE) HC**	**LSM(SE)HR**	**P value**	**LSM(SE) HC**	**LSM(SE)HR**	**P value**
Arc_FT_L	0.3679 (0.00231)	0.3580 (0.00426)	0.03 *	0.0013 (0.00000)	0.0013 (0.00001)	0.08	0.0007 (0.00000)	0.0008 (0.00001)	0.13
Arc_FT_R	0.3476 (0.00218)	0.3424 (0.00400)	0.24	0.0013 (0.00000)	0.0013 (0.00001)	0.41	0.0008 (0.00000)	0.0008 (0.00001)	0.42
Cing_G_L	0.3074 (0.00221)	0.3038 (0.00406)	0.42	0.0013 (0.00000)	0.0013 (0.00001)	0.25	0.0008 (0.00000)	0.0008 (0.00001)	0.95
Cing_G_R	0.2934 (0.00238)	0.2963 (0.00438)	0.55	0.0013 (0.00000)	0.0013 (0.00001)	0.50	0.0008 (0.00000)	0.0008 (0.00001)	0.90
Cing_H_L	0.2898 (0.00183)	0.2792 (0.00334)	<0.01 **	0.0012 (0.00000)	0.0012 (0.00001)	0.02 *	0.0008 (0.00000)	0.0008 (0.00000)	0.17
Cing_H_R	0.2765 (0.00171)	0.2740 (0.00315)	0.46	0.0012 (0.00000)	0.0012 (0.00001)	0.70	0.0008 (0.00000)	0.0008 (0.00000)	0.62
CT_Pre_FL	0.2537 (0.00125)	0.2532 (0.00230)	0.83	0.0012 (0.00000)	0.0012 (0.00001)	0.51	0.0008 (0.00000)	0.0008 (0.00001)	0.80
CT_Pre_FR	0.2979 (0.00130)	0.2967 (0.00239)	0.64	0.0013 (0.00000)	0.0013 (0.00001)	0.55	0.0008 (0.00000)	0.0008 (0.00001)	0.49
ILF_L	0.3890 (0.00249)	0.3851 (0.00459)	0.45	0.0015 (0.00001)	0.0014 (0.00001)	0.36	0.0008 (0.00000)	0.0008 (0.00001)	0.97
ILF_R	0.3801 (0.00226)	0.3776 (0.00416)	0.59	0.0014 (0.00001)	0.0014 (0.00001)	0.32	0.0008 (0.00000)	0.0008 (0.00001)	0.92
SLF_L	0.3094 (0.00211)	0.3076 (0.00388)	0.67	0.0013 (0.00000)	0.0013 (0.00001)	0.36	0.0008 (0.00000)	0.0008 (0.00001)	0.36
SLF_R	0.3128 (0.00235)	0.3086 (0.00441)	0.40	0.0013 (0.00000)	0.0013 (0.00001)	0.87	0.0008 (0.00000)	0.0008 (0.00001)	0.31
IFOF_L	0.3874 (0.00212)	0.3837 (0.00390)	0.39	0.0014 (0.00001)	0.0014 (0.00001)	0.50	0.0008 (0.00000)	0.0008 (0.00001)	0.71
IFOF_R	0.3919 (0.00210)	0.3892 (0.00392)	0.52	0.0014 (0.00000)	0.0014 (0.00001)	0.67	0.0007 (0.00000)	0.0007 (0.00001)	0.49
UNC_L	0.3074 (0.00149)	0.3037 (0.00279)	0.23	0.0013 (0.00000)	0.0013 (0.00001)	0.30	0.0008 (0.00000)	0.0008 (0.00000)	0.09
UNC_R	0.3479 (0.00172)	0.3455 (0.00316)	0.48	0.0013 (0.00000)	0.0014 (0.00001)	0.25	0.0008 (0.00000)	0.0008 (0.00000)	0.16
CC_Genu	0.4433 (0.00237)	0.4381 (0.00436)	0.28	0.0015 (0.00000)	0.0016 (0.00001)	0.12	0.0007 (0.00000)	0.0007 (0.00001)	0.21
CC_Splen	0.4569 (0.00221)	0.4536 (0.00407)	0.47	0.0015 (0.00000)	0.0015 (0.00001)	0.93	0.0007 (0.00000)	0.0007 (0.00001)	0.84

FA, fractional anisotropy; AD, axial diffusivity; RD, radial diffusivity; LSM, least square mean; SE, standard error

Arc_FT_L, left arcuate front-temporal fasciculus; Arc_FT_R, right arcuate front-temporal fasciculus; Cing_G_L, left cingulate superior segment; Cing_G_R, right cingulate superior segment; Cing_H_L, left cingulate hippocampal segment; Cing_H_R, right cingulate hippocampal segment; CT_PreF_L, left prefronal corticothalamic tract; CT_PreF_R, right prefronal cortico-thalamic tract; ILF_L, left inferior longitudinal fasciculus; ILF_R, right inferior longitudinal fasciculus; SLF_L, left superior longitudinal fasciculus; SLF_R, right superior longitudinal fasciculus; IFOF_L, left inferior fronto-occipital fasciculus; IFOF_R, right inferior fronto-occipital fasciculus; UNC_L, left uncinated fasciculus; UNC_R, right uncinated fasciculus; CC_Genu, callosal genu; CC_Splen, callosal splenium

* $p < 0.05$;

** $p < 0.01$;

† $p < 0.05$ after FDR correction

Table 5.

Comparison of least square means of DTI metrics of 18 white matter tract between two year olds at risk for schizophrenia and healthy controls. The model 1 was adjusted by gestational age at birth, gender, postnatal age at MRI, and MRI scanner type.

	FA			AD			RD		
Tract	**LSM(SE) HC**	**LSM(SE)HR**	**P value**	**LSM(SE) HC**	**LSM(SE)HR**	**P value**	**LSM(SE) HC**	**LSM(SE)HR**	**P value**
Arc_FT_L	0.4130 (0.00293)	0.4019 (0.00457)	0.03 *	0.0013 (0.00000)	0.0013 (0.00001)	0.42	0.0007 (0.00000)	0.0007 (0.00001)	0.09
Arc_FT_R	0.3973 (0.00284)	0.3879 (0.00443)	0.07	0.0013 (0.00000)	0.0013 (0.00001)	0.99	0.0007 (0.00000)	0.0007 (0.00001)	0.03 *
Cing_G_L	0.3570 (0.00283)	0.3492 (0.00442)	0.13	0.0013 (0.00001)	0.0013 (0.00001)	0.42	0.0007 (0.00000)	0.0007 (0.00001)	0.22
Cing_G_R	0.3387 (0.00336)	0.3384 (0.00523)	0.94	0.0012 (0.00001)	0.0012 (0.00001)	0.62	0.0007 (0.00000)	0.0007 (0.00001)	0.79
Cing_H_L	0.3165 (0.00261)	0.3042 (0.00407)	0.01 *	0.0012 (0.00000)	0.0012 (0.00001)	0.30	0.0007 (0.00000)	0.0007 (0.00001)	0.08
Cing_H_R	0.3091 (0.00289)	0.3006 (0.00451)	0.10	0.0012 (0.00000)	0.0011 (0.00001)	0.76	0.0007 (0.00000)	0.0007 (0.00000)	0.12
CT_PreF_L	0.2852 (0.00177)	0.2767 (0.00276)	<0.01 **	0.0012 (0.00000)	0.0012 (0.00001)	0.92	0.0008 (0.00000)	0.0008 (0.00001)	0.15
CT_Pre_FR	0.3330 (0.00194)	0.3282 (0.00302)	0.17	0.0013 (0.00000)	0.0013 (0.00001)	0.49	0.0007 (0.00000)	0.0007 (0.00000)	0.37
ILF_L	0.4403 (0.00333)	0.4343 (0.00519)	0.32	0.0014 (0.00001)	0.0014 (0.00001)	0.74	0.0007 (0.00000)	0.0007 (0.00001)	0.40
ILF_R	0.4262 (0.00301)	0.4192 (0.00469)	0.20	0.0014 (0.00001)	0.0014 (0.00001)	0.60	0.0007 (0.00000)	0.0007 (0.00001)	0.47
SLF_L	0.3538 (0.00300)	0.3428 (0.00468)	0.04 *	0.0012 (0.00001)	0.0012 (0.00001)	0.69	0.0007 (0.00000)	0.0007 (0.00001)	0.02 *
SLF_R	0.3538 (0.00315)	0.3426 (0.00479)	0.04 *	0.0012 (0.00001)	0.0012 (0.00001)	0.81	0.0007 (0.00000)	0.0007 (0.00001)	0.03 *
IFOF_L	0.4385 (0.00298)	0.4307 (0.00465)	0.15	0.0014 (0.00001)	0.0014 (0.00001)	0.75	0.0007 (0.00000)	0.0007 (0.00001)	0.18
IFOF_R	0.4416 (0.00272)	0.4335 (0.00423)	0.10	0.0014 (0.00001)	0.0014 (0.00001)	0.82	0.0007 (0.00000)	0.0007 (0.00001)	0.17
UNC_L	0.3423 (0.00222)	0.3356 (0.00345)	0.09	0.0012 (0.00000)	0.0013 (0.00001)	0.33	0.0007 (0.00000)	0.0007 (0.00001)	0.06
UNC_R	0.3901 (0.00278)	0.3847 (0.00431)	0.28	0.0013 (0.00001)	0.0013 (0.00001)	0.21	0.0007 (0.00000)	0.0007 (0.00001)	0.07
CC_Genu	0.5070 (0.00290)	0.5060 (0.00453)	0.86	0.0015 (0.00001)	0.0015 (0.00001)	0.92	0.0006 (0.00000)	0.0006 (0.00001)	0.82
CC_Splen	0.4980 (0.00280)	0.4908 (0.00437)	0.15	0.0015 (0.00001)	0.0015 (0.00001)	0.5101	0.0006 (0.00000)	0.0006 (0.00001)	0.16

FA, fractional anisotropy; AD, axial diffusivity; RD, radial diffusivity; LSM, least square mean; SE, standard error

Arc_FT_L, left arcuate front-temporal fasciculus; Arc_FT_R, right arcuate front-temporal fasciculus; Cing_G_L, left cingulate superior segment; Cing_G_R, right cingulate superior segment; Cing_H_L, left cingulate hippocampal segment; Cing_H_R, right cingulate hippocampal segment; CT_PreF_L, left prefronal corticothalamic tract; CT_PreF_R, right prefronal cortico-thalamic tract; ILF_L, left inferior longitudinal fasciculus; ILF_R, right inferior longitudinal fasciculus; SLF_L, left superior longitudinal fasciculus; SLF_R, right superior longitudinal fasciculus; IFOF_L, left inferior fronto-occipital fasciculus; IFOF_R, right inferior fronto-occipital fasciculus; UNC_L, left uncinated fasciculus; UNC_R, right uncinated fasciculus; CC_Genu, callosal genu; CC_Splen, callosal splenium

* $p < 0.05$;

** $p < 0.01$;

Author Manuscript

Author Manuscript

Author Manuscript

$^{\dagger}p < 0.05$ after FDR correction

Table 6.

Comparison of two general linear models in significant least square mean difference between neonates at high risk for schizophrenia and healthy control. The model 1 was adjusted for gestational age at birth, gender, postnatal age at MRI, and MRI scanner type. Model 2 was adjusted by model 1 covariate plus maternal education. Non-significant tracts are not shown.

	Neonates		Model 1 One year		Two year		Neonates		Model 1 + maternal education One year		Two year	
Tract	**V**	**P-value**	**V**	**P-value**	**V**	**P-value**	**V**	**P-value**	**V**	**P-value**	**V**	**P-value**
Arc_FT_L	FA	0.36	FA	0.03*	FA	0.03*	FA	0.80	FA	0.14	FA	0.36
	AD	0.86	AD	0.08	AD	0.42	AD	0.46	AD	0.13	AD	0.63
	RD	0.43	RD	0.13	RD	0.09	RD	0.83	RD	0.21	RD	0.66
Cing_G_L	FA	0.03*	FA	0.42	FA	0.13	FA	0.02*	FA	0.96	FA	0.06
	AD	0.20	AD	0.25	AD	0.42	AD	0.03*	AD	0.42	AD	0.46
	RD	0.99	RD	0.95	RD	0.22	RD	0.56	RD	0.54	RD	0.11
Cing_H_L	FA	0.05	FA	<0.01**	FA	0.01*	FA	0.22	FA	<0.01**	FA	0.09
	AD	0.13	AD	0.02*	AD	0.30	AD	0.30	AD	0.02*	AD	0.28
	RD	<0.01**	RD	0.17	RD	0.08	RD	0.04*	RD	0.22	RD	0.53
CT_PreF_L	FA	0.53	FA	0.83	FA	<0.01**	FA	0.62	FA	0.56	FA	0.04*
	AD	0.23	AD	0.51	AD	0.92	AD	0.63	AD	0.69	AD	0.91
	RD	0.27	RD	0.80	RD	0.15	RD	0.89	RD	0.79	RD	0.25
SLF_L	FA	0.85	FA	0.67	FA	0.04*	FA	0.80	FA	0.57	FA	0.08
	AD	0.74	AD	0.36	AD	0.69	AD	0.73	AD	0.95	AD	0.89
	RD	0.72	RD	0.36	RD	0.02*	RD	0.77	RD	0.59	RD	0.07
SLF_R	FA	0.51	FA	0.40	FA	0.04*	FA	0.79	FA	0.96	FA	0.19
	AD	0.52	AD	0.87	AD	0.81	AD	0.12	AD	0.70	AD	0.61
	RD	0.69	RD	0.31	RD	0.03*	RD	0.18	RD	0.68	RD	0.12
UCN_R	FA	0.03*	FA	0.48	FA	0.28	FA	0.60	FA	0.63	FA	0.30
	AD	0.25	AD	0.25	AD	0.21	AD	0.74	AD	0.56	AD	0.31
	RD	0.10	RD	0.16	RD	0.07	RD	0.74	RD	0.43	RD	0.04*

V, variable; Arc_FT_L, left arcuate front-temporal fasciculus; Cing_G_L, left cingulate superior segment; Cing_H_L, left cingulate hippocampal segment; CT_PreF_L, left prefronal cortico-thalamic tract; SLF_L, left superior longitudinal fasciculus; SLF_R, right superior longitudinal fasciculus; UNC_R, right uncinated fasciculus.

* $p < 0.05$;
** $p < 0.01$